Mirror twin boundaries in WSe2 induced by vanadium doping

Pathirage, V.; Lasek, K.; Krasheninnikov, A.; Komsa, H. P.; Batzill, M.;

Originally published:

January 2023

Materials Today Nano 22(2023), 100314

DOI: https://doi.org/10.1016/j.mtnano.2023.100314

Perma-Link to Publication Repository of HZDR:

https://www.hzdr.de/publications/Publ-36905

Mirror twin boundaries in WSe_2 induced by vanadium doping

Vimukthi Pathirage,[1] Kinga Lasek,[1] Arkady V. Krasheninnikov,[2,3] H.P. Komsa,[4] Matthias Batzill[1]

[1]Department of Physics, University of South Florida, Tampa, FL 33620, USA

[2] Helmholtz-Zentrum Dresden-Rossendorf, Institute of Ion Beam Physics and Materials Research, 01328 Dresden, Germany

[3]Department of Applied Physics, Aalto University, P.O. Box 11100, 00076 Aalto, Finland

[4]Microelectronics Research Unit, University of Oulu, P.O. Box 8000, Oulu 90014, Finland

Abstract:

Mirror twin boundaries (MTBs) observed in $MoSe_2$ are formed due to incorporation of excess Mo into the lattice. In contrast, MTBs in WSe_2 have a high formation energy and consequently are not present in this system. Here we show that V-doping of WSe_2, achieved by co-deposition of V and W during molecular beam epitaxy (MBE) growth of WSe_2, can also induce MTB formation in WSe_2, as revealed by scanning tunneling microscopy. Our experimental results are supported by density functional theory calculations that show that V-doped WSe_2 is susceptible to the incorporation of more V-atoms at interstitial sites. This increases the transition metal atom concentration in the lattice, and these excess atoms rearrange into MTBs, which is associated with energy lowering of the excess metal atoms. While formation of MTBs gives rise to the pinning of the Fermi-level and thus prevents V-induced electronic doping, MTBs do not appear to affect the magnetic properties, and a diluted ferromagnetic material is observed for low V-doping levels, as reported previously for V-doped WSe_2.

Group VIB transition metal dichalcogenides, specifically the 2H- Mo- and W- systems are among the prototypical two-dimensional (2D) semiconductors. Most of their fundamental properties and device performances have been studied by exfoliation of individual structural units from their respective bulk materials. However, direct growth methods are required for low-cost production of these materials to enable applications and importantly to modify their properties with dopants. Molecular beam epitaxy (MBE) and related physical vapor deposition methods are significant growth methods that enable their synthesis as mono- to few-layer films and to integrate them in van der Waals (vdW) heterostructures.[1,2] Thin films grown by direct growth methods, generally exhibit higher defect concentrations compared to bulk crystals. In addition, defect formation mechanisms in 2D materials can be significantly different from those in traditional materials that form 3D crystal structures. In the so called vdW epitaxy,[3] the weak vdW interactions with the substrate prevent the formation of interface misfit defects. However, the lack of 3D bonding networks in 2D materials also implies less constraints on the crystal structure and therefore easier crystal modifications. This has been observed for the 2H-Mo dichalcogenides, that can exhibit an abundance of mirror twin boundaries (MTBs) between the grains in grown films.[4,5,6,7,8,9,10] In $MoSe_2$ and $MoTe_2$, MTBs are observed as closed triangular loops or dense networks of line defects.[11,12,13] In contrast, in MoS_2, MTBs are only observed as boundaries of merging grains.[14,15] This indicates that there are different formation mechanisms for MTBs in these materials.[16] Systematic experimental and theoretical studies have shown that excess Mo is readily incorporated into interstitial sites of $MoSe_2$ and $MoTe_2$, but not of MoS_2.[17] It is the interstitials, or excess Mo-atoms, that are being converted into MTB triangular loops, as schematically illustrated in Fig. S1. The difference between MoS_2 and $MoTe_2$/$MoSe_2$ is the energy cost for incorporating excess Mo into the lattice, at interstitial sites. Like MoS_2, WSe_2 also does not readily incorporate excess W and the formation energy of MTBs in WSe_2 is high.[18] Thus, the formation of MTBs in pure WSe_2 is unfavorable and consequently MBE grown WSe_2 films are free of MTB loops.[19,20,21,22] However, while incorporation of excess Mo- or W- atoms may be unfavorable, this does not exclude the possibility for hetero-atoms to be incorporated at interstitial sites. The incorporation of such hetero-atoms has been discussed theoretically for Mo-dichalcogenides[23] and has been demonstrated experimentally.[24] This raises the question if hetero-transition metals may be incorporated into WSe_2 during growth and if this can lead to MTB formation in this material. To study this, we co-deposit vanadium and tungsten with selenium in an MBE chamber and characterize the grown materials with STM. While pure WSe_2 is free of MTBs, the V-doped samples exhibit high density of MTB grains and grain boundary loops. This indicates that excess TM can be incorporated in V-doped WSe_2 (in excess of the TM-dichalcogenide composition) and consequently this can trigger the formation of MTBs also in WSe_2. DFT calculations clarify the mechanism and role of V in the formation of MTBs in WSe_2.

MTBs in TMDs are exciting crystal modifications as they exhibit truly one-dimensional metallic properties embedded in a semiconducting host material. As such, it has been shown that these MTBs exhibit Tomonaga Luttinger quantum liquid behavior and consequently separate spin- and charge- excitation, generally known as the separation of spin- and charge- degrees of freedom, are observed in MTBs in Mo-dichalcogenides.[6,15] The formation of MTBs in WSe_2 expands this family of MTBs and will enable tuning and further investigation of their electronic properties. In a more applied sense, MTBs have been shown to be potentially active sites for electrocatalytic hydrogen evolution reactions[25] and thus introducing their formation in TMDs that do not easily form MTBs intrinsically is an important step for making novel catalytic materials. In some cases, a very high-density a MTB network may be achieved, and such uniform arrangements of MTBs may be considered a new 2D material.[26] In many applications, however, defect formation may be undesirable. Therefore, a detailed understanding of the defect formation mechanisms

is required to counteract their formation. In this respect, the findings reported here that the incorporation of impurity dopants can facilitate the formation of MTBs in WSe_2 is of relevance for controlling the synthesis of 2D materials.

Detailed information on technical aspects of sample preparation, sample characterization and analysis, and computation can be found in the supplementary information. Figure 1 shows STM images of pure WSe_2 grown at 400˚C on an HOPG substrate. The pristine samples without dopants consist of monolayer islands with some bi- and multilayer regions. Atomically resolved images of the monolayer regions reveal a moiré structure due to the lattice-misfit between the substrate and the WSe_2 lattices. In large scale STM images the island edges appear bright, an indication of their metallic nature, which is generally observed for WSe_2 and MoX_2 (X= S, Se, Te).[27,28,29,30] In addition, some bright grain boundaries are observed that form because of rotational misalignment between the grains. Importantly though, there are only very rare indications of twin grain boundaries in these undoped samples.[22] In addition we varied the growth conditions by varying the growth temperature or the W-flux, *i.e.*, the W:Se ratio. STM images, shown in Fig. S4, indicate that MTBs are not formed in pristine WSe_2 over the whole range of accessible growth conditions.

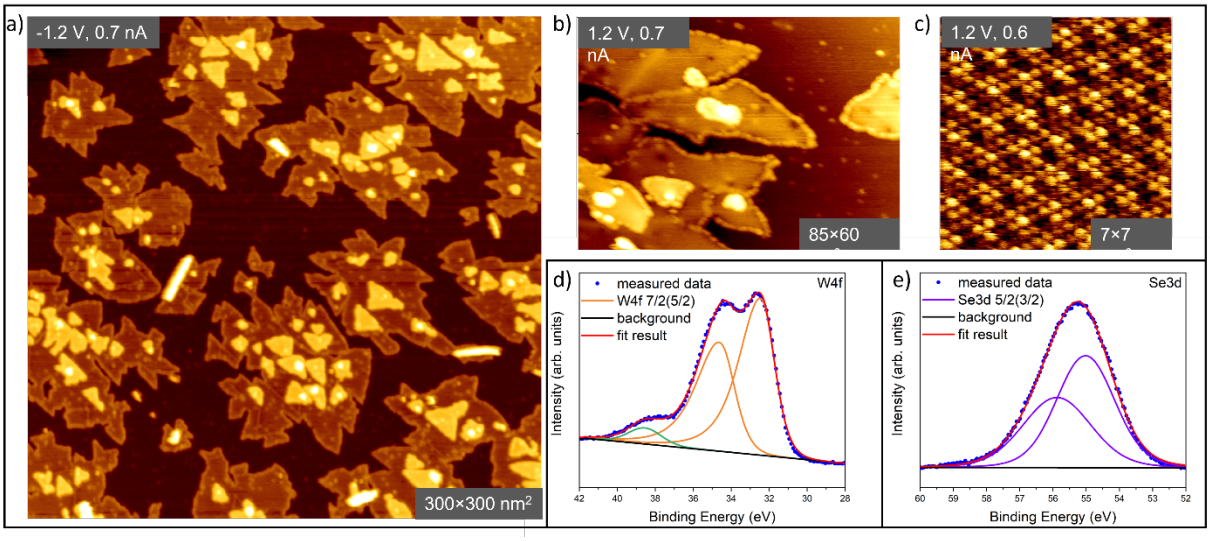

Fig. 1: STM and XPS characterization of pure WSe_2 grown on HOPG substrate. (a) large scale STM image showing the island structure with bare HOPG in between the WSe_2 islands. Some bilayer regions and isolated trilayers can be found. (b) at a smaller scale bright edges of the WSe_2 islands are apparent. These bright edges are associated with band gap states at the edges. (c) atomic resolution images of the WSe_2 monolayer shows a moiré structure but few atomic scale defects. The W-4f and Se-3d core level spectra are shown in (d) and (e), respectively.

Samples with different vanadium concentration were grown, and the sample morphology changes dramatically when vanadium is co-deposited with tungsten, which is shown in Fig. 2. In this case the sample exhibits straight line-defects that form preferentially triangular closed loops or a crisscrossing network of lines at 60-degree angles relative to each other. These line defects are best observed at below -1.3 V bias voltage (see supplement Fig. S2), *i.e.*, tunneling conditions close to the band edge of the semiconducting pristine WSe_2. At these tunneling conditions the line defects appear as bright double rows. The structure and appearance in STM are in analogy to that of MTBs observed in $MoSe_2$ and $MoTe_2$

and thus are assigned as such. The double row appearance arises from the higher tunneling probabilities at the Se-sites adjacent to the MTB, as has been confirmed by simulated STM images for $MoSe_2$.[17] In between the MTBs the same moiré structure as for the pristine WSe_2 monolayers can be observed. High resolution STM images are shown in Fig. S3. The amount of vanadium in the samples have been determined from XPS. Fig. 2 shows XPS of W-4f and V-2p for different samples and corresponding STM images. For all samples the W $4f_{7/2}$ binding energy is measured as 32.47 ± 0.02 eV. The lack of any shift in the W-4f binding energy with or without V-doping, suggesting that there is no significant change of the Fermi-level position within the band gap of WSe_2. The metallic MTBs in $MoSe_2$ and $MoTe_2$ have been shown to pin the Fermi-level around mid-gap[13,17] and similar Fermi-level pinning is expected for MTB-modified WSe_2 so that V-induced p-doping is prevented.

The MTB networks are inhomogeneous across the sample, with some areas exhibiting very dense networks while others only show isolated triangular loops. This inhomogeneity may suggest that the formation of MTBs is not determined by the uniform flux of V and W on the surface but may be a consequence of post-growth incorporation of vanadium into the sample. Such processes were invoked for MTB formation in $MoSe_2$/$MoTe_2$ for which post-growth incorporation of Mo was shown to cause MTB formation.[16,17] Thus, WSe_2 regions that have grown first will have been exposed to more vanadium during growth and thus more vanadium can be incorporated resulting in formation of denser MTB networks in these areas. An analysis of the MTB density (total length of the MTBs per unit area) is presented in Fig. S5 for the samples shown in Fig. 2. With increasing vanadium concentration, we also observe the formation of secondary phase at the edges of the grown WSe_2 islands. This secondary phase along the edges is only observed for high V-concentrations above ~10%. This suggests that the vanadium solubility in WSe_2 is limited and if the concentration is becoming too high the V is pushed out of the growing island where it forms a phase with high vanadium concentration along the edges of the WSe_2 islands. In Fig. 2(c) this is clearly observed by a bright rim that decorates the monolayer islands. See also Fig. S6 to help distinguish between MTB networks and secondary phase. The bright contrast may suggest that this phase is metallic or has a much smaller band gap than WSe_2. Also note that the width of the bright contrast around the island edges of this secondary phase is ~5 nm (see Fig. S6) and thus much wider than the atomic scale bright edges observed for pure WSe_2 islands. It would be desirable to identify the atomic position of the V-dopants in these samples. However, our STM imaging does not unambiguously distinguish between defects such as Se-vacancies and V-impurities. Some bright protrusions that are visible in the STM images for doped samples are also observed in pristine WSe_2 samples (Fig.1) and thus may not be associated with V-dopants. A recent study of V:WSe_2, grown under similar conditions as shown here, also report scanning transmission electron microscopy which helped to identify V-dopants substituting for W-atoms as well as V-atoms within the MTBs.[31] We may expect similar V-distribution in the samples reported here.

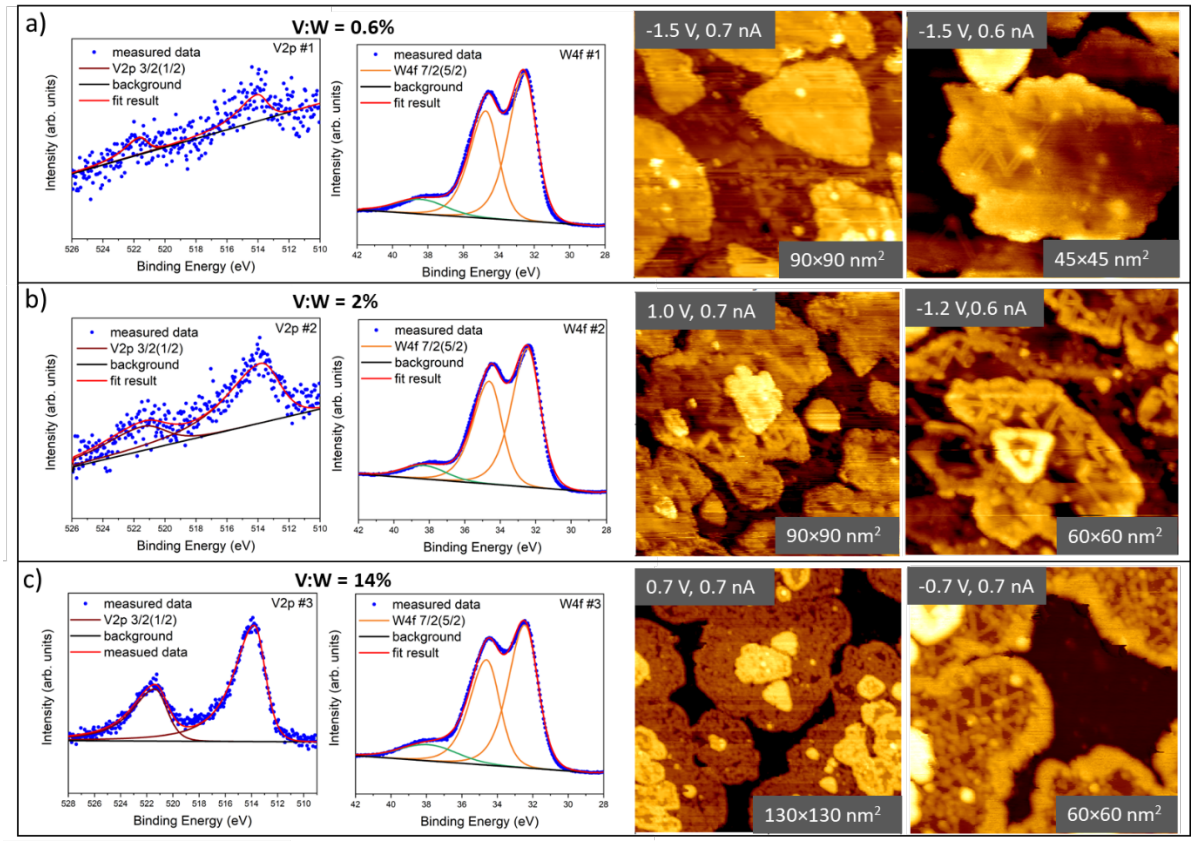

Fig. 2: XPS and STM characterization of V-doped WSe_2. The V concentration increases from (a) 0.6 %, (b) 2%, to (c) 14 %.

Several studies of vanadium doped WSe_2 have report ferromagnetic properties and thus V:WSe_2 system has been suggested to be a 2D diluted magnetic semiconductor.[32,33,34] The saturation magnetization for V:WSe_2 in CVD grown samples have been shown to reach a maximum for ~4 at% doping and for larger amount the magnetization disappears, which may be related to a solubility limit of V in WSe2.[35] Fig. 3 shows vibrating sample magnetometry (VSM) measurements on three samples grown by MBE. The un-doped WSe_2 sample does not show any significant magnetization with a very small signal associated with defects. For a sample doped with a vanadium concentration of ~2 at% shows the highest saturation magnetization, which then drops almost back to zero for the higher doped sample at 12 at%. This is consistent with previous reports for dopant induced magnetization in WSe_2. Also, the magnetization characteristics of a narrow hysteresis loop with a coercive field of only 140 Oe and persistence of the magnetization to RT is similar to the reported data. The growth of V-doped WSe_2 by MBE is significantly different from that reported previously which was done by CVD growth. The lower growth temperature in MBE may enable a higher V-concentration. Most importantly TEM investigation of CVD grown samples does not show the formation of MTB-networks. This is similar to observations for Mo-dichalcogenides where MTB networks are only commonly observed in MBE growth, suggesting that a lower growth temperature is important to obtain MTB networks. Similar trends for the magnetic properties with V-concentration between CVD and MBE grown samples, however, suggest that the MTB networks are not significantly influencing the magnetic properties. While this agrees with our expectation that V is randomly incorporated into the WSe_2 lattice and is not primarily located in the MTBs, the Fermi-level

position of WSe_2 is anticipated to be affected by MTBs. The metallic mid-gap states of the MTBs pin the Fermi-level and thus prevent a p-type doping of WSe_2 as shown for CVD grown samples.[36,37] An enhancement of magnetic ordering by post-growth annealing induced Se-vacancies has been recently reported,[38] and the electron transfer from MTB networks may have similar magnetism enhancing effects as proposed for Se-vacancies.

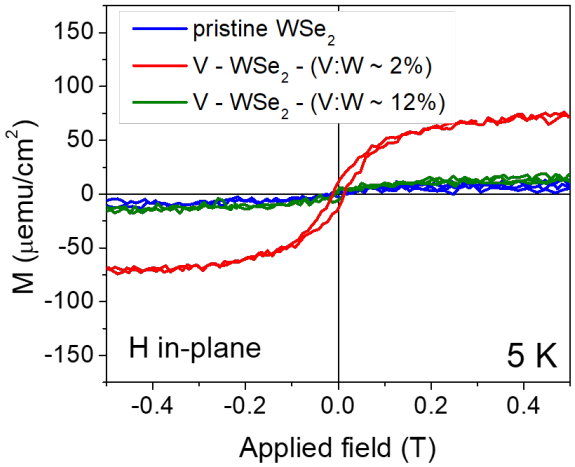

Fig. 3: Magnetization versus applied magnetic field hysteresis plots taken at 5K for 3 different samples. Pristine WSe_2 and a sample doped with 12% V show negligible magnetization, while the sample with 2% V doping exhibits magnetization with a small (140 Oe) coercive field.

In order to understand the mechanism behind the formation of a high-density MTB network, we simulated the relevant atomic processes using density-functional theory (DFT) calculations. First, the existence of MTBs necessitates sample stoichiometry with excess metal atoms (or selenium deficiency). Formation of MTB networks directly at the growth front during expansion of the islands seems unlikely, since the network appears independent of the edge details and there should be different mechanisms for forming the MTBs parallel and perpendicular to the edge. Thus we consider transformations in the sample interior by incorporation of excess metal atoms, as was demonstrated for MTB formation in $MoSe_2$ and $MoTe_2$.[17] In this previous work on MTBs of Mo-dichalcogenides, Mo-atoms were deposited on pristine surfaces and we proposed a mechanism wherein the metal atoms are first absorbed into interstitial sites and then a transformation to MTB loops occurs as several excess Mo-atoms interact.[17] Modeling MBE growth using DFT is challenging since we cannot assume equilibrium conditions as the temperature is relatively low (compared to CVD or other growth methods) and the process may be affected by the kinetics. However, low energy configurations are still preferred as long as there exists a viable kinetic pathway.

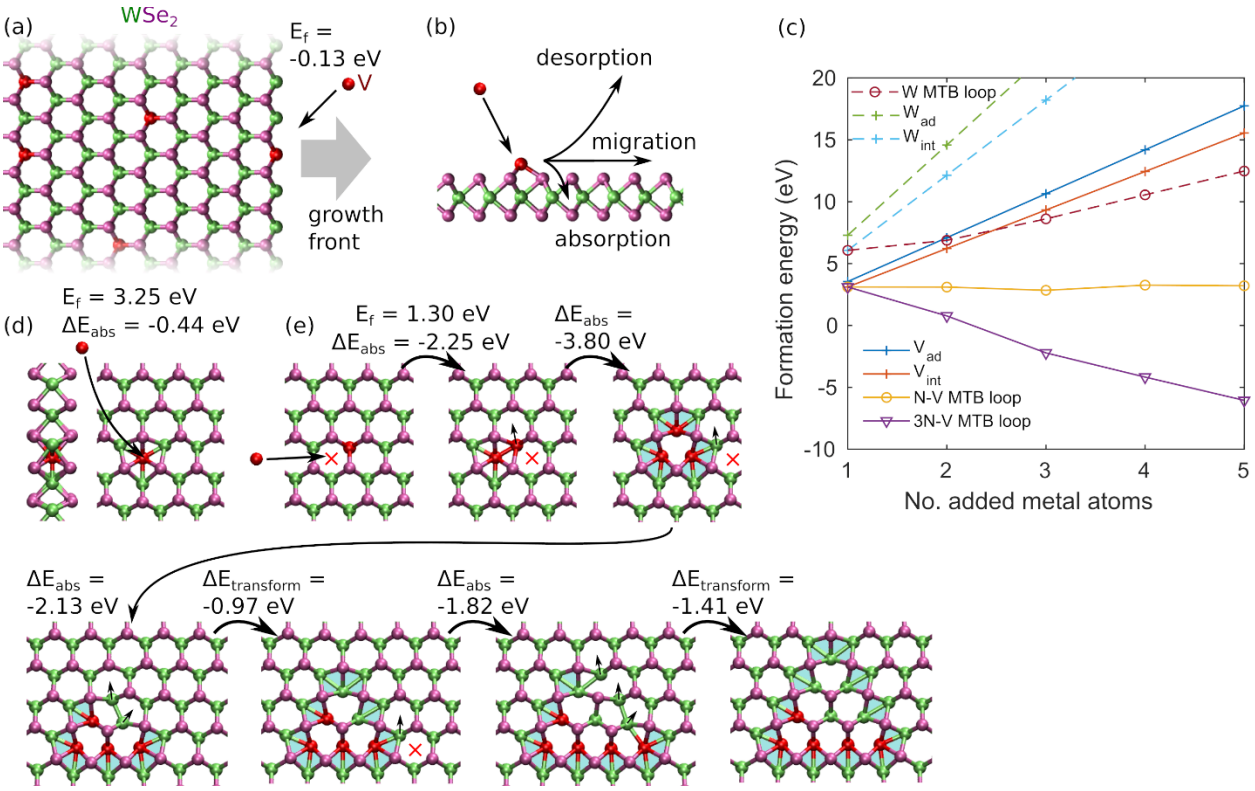

Fig. 4: (a,b) Illustration of the process for incorporation of V in W-sites during the propagation of the growth front (a) and some possible processes for V adatoms (b). (c) Formation energy of various types of defects as a function of the number of added metal atoms. Here W_{ad} stands for extra W atoms in the adatom positions, W_{int} for W interstitials, V_{ad} and V_{int} stand for extra V atoms in the adatom and interstitial positions, and W-MTB, N-V and 3N-V MTB correspond to MTB loops consisting of only W or containing N or 3N V atoms. (d) Structure and energies of V interstitial. (e) Evolution of the structure from isolated point defects to MTB loops and corresponding energy differences. Red cross denotes the site at which V interstitial is absorbed and small black arrows denote the movement of neighboring metal atoms.

In Fig. 4(a,b) we illustrate the relevant processes, and in Fig. 4(c) we show the formation energies of various types of defects (adatoms W_{ad}/V_{ad}, interstitials W_{int}/V_{int}, and MTB loops consisting of only W or containing *N* or *3N* V atoms) as functions of the number of metal atoms added to the system (and calculated under metal-rich conditions, see also Table S1 for numerical values under different conditions). Based on the calculated values, we propose the following mechanism: (i) V atoms arriving at the growth front can be incorporated into the lattice as substitutional V@W defects, as illustrated in Fig. 4(a). The formation energy of V@W configuration is -0.13 eV, *i.e.*, being negative it is limited only by the V supply. (ii) V (or some molecules involving V, W, and/or Se) landing on the surface can migrate to edges, desorb, or absorb into interstitial sites, Fig. 4(b). The lowest energy configuration for an additional V atom is at the interstitial site, -0.44 eV lower than adatom-site, and thus such configuration is favored. In practice, if equilibrium can be assumed, the concentration of interstitials might still be low due to the relatively high formation energy of 3.25 eV, Fig. 4(d). However, when V@W already exists in the lattice, the formation energy decreases dramatically to 1.30 eV, 0.42 eV, and -0.17 eV for 1, 2, and 3 V@W defects in the neighboring lattice sites, respectively, Fig. 4(e). That is, pre-existing V@W make the absorption of V into the interstitial sites of the lattice more probable. In contrast, without pre-existing V@W defects, V

incorporation is energetically prohibitive, and V is expected to remain at the surface. This can be tested experimentally by V-deposition on pristine WSe_2 islands. It is found that on such islands V forms V-clusters (see Fig. S7). (iii) Finally, the MTBs can form and expand in the same way as proposed in our previous work.[17] In Figure 4(e) we demonstrate one possible pathway and the related energy differences. First, addition of second V interstitial next to the $V@W+V_{int}$ yields a spontaneous transformation to the minimal MTB loop that will act as a seed for further growth. When more V interstitials are added, the structure is distorted towards the MTB loop structure, but an additional step is required to complete the transformation. Nevertheless, all the steps show marked energy lowering.

As shown in Fig. 4(c), the formation energy of the V-containing MTB loops remains low. "N-V MTB loop" refers to a case where all additional atoms required to grow the MTB loop arise from absorbed V, in which case *N* V atoms are needed for the MTB loop with edge length of *N* lattice constants (or, correspondingly, about 1/6 of the total atoms in the loop are V). The formation energy remains nearly constant, meaning that there is essentially no energy cost involved in increasing the size of the MTB loop after the seed is formed. Moreover, if additional V is present in the MTB loop, the formation energy can be further lowered, as shown in the "3N-V MTB loop" case where half of the MTB atoms are V. The formation energies in Fig. 4(c) also demonstrate why MTB loops are unlikely when W is the only metal species. First, the formation energies of isolated W defects are much higher than those of the corresponding V defects, and importantly the lowest energy configuration is found for the W-sub defect (Table S1), thus limiting absorption to the interstitial sites. Second, the MTB loop formation energies without V are much higher than with V and increasing with the size of the MTB loop. Also the induced stress on the supercell is clearly smaller with V, the main reason for much smaller formation energies of V-containing MTBs is the smaller ionic radii of V and thus reduced strain after incorporating additional metal atoms into the lattice.

In conclusion, MTBs in pristine WSe_2 have a large formation energy[18] and consequently are not observed in MBE grown pure WSe_2 films. In contrast, V-doping of WSe_2 in MBE growth triggers the formation of MTBs and thus the inclusion of substantial V (V@W) modifies the growth process of WSe_2. Our DFT calculations reveal that substitutional V-atoms in WSe_2 lower the formation energies for V-interstitials, and this facilitates V-adatoms to be absorbed at interstitial sites. These additional V-atoms in the WSe_2 lattice can then evolve into MTBs and 'capture' additional V-atoms that are deposited on the surface during the growth process. The growth of the MTB-loops does not cost any energy and thus, once nucleated, they will grow as more V-atoms are incorporated. This mechanism explains the formation of MTB networks observed in the experiments when V and W are co-deposited in a Se-background. This behavior of V is consistent with recent reports for Nb-deposition on WSe_2 (Nb is p-type dopant in WSe_2) that showed that Nb can diffuse into WSe_2 and replace W.[39,40] The MTB formation in WSe_2 may be compared to $MoSe_2$ or $MoTe_2$ which do not require impurity atoms for MTB formation. The difference is that in $MoSe_2$ or $MoTe_2$ vapor deposited excess Mo can be incorporated into interstitial sites and thus induce MTB formation, while this process is energetically prohibited for W-atoms in WSe_2. Thus, to obtain an excess TM-concentration in WSe_2, which then can rearrange into MTBs, an impurity TM is needed. We note that V atoms in MTBs do not have magnetic moments according to our calculations, and thus do not affect magnetic properties of the V-doped WSe_2 samples, and the observed magnetization originates from isolated V impurities. For Mo-dichalcogenides, the propensity of TM to incorporate into the 2D lattice has been screened by DFT calculations for all the TMs,[23] a similar computational approach for WSe_2 may give guidance to which elements may be incorporated into WSe_2, in addition to V and Nb.

Declaration of competing interest

The authors declare that they have no known competing financial interests or personal relationships that could have appeared to influence the work reported in this paper.

Acknowledgement: Financial support from the National Science Foundation under award DMR 2118414 is acknowledged. We further acknowledge funding from the German Research Foundation (DFG), project KR 4866/6-1, and through the collaborative research center "Chemistry of Synthetic 2D Materials" SFB-1415- 417590517. The authors wish to acknowledge CSC – IT Center for Science, Finland, for computational resources. We also thank the Gauss Centre for Supercomputing e.V. (www.gauss-centre.eu) for providing computing time on the GCS Supercomputer HAWK at Höchstleistungsrechenzentrum Stuttgart (www.hlrs.de) and also TU Dresden (Taurus cluster) for generous grants of CPU time.

Appendix A. Supplementary data

Supplementary data to this article can be found online at https://doi.org/ XXXX

References:

[1] M.I.B. Utama, Q. Zhang, J. Zhang, Y. Yuan, F.J. Belarre, J. Arbiol, and Q. Xiong, Recent developments and future directions in the growth of nanostructures by van der Waals epitaxy. Nanoscale 5 (2013) 3570-3588.

[2] K. Lasek, J. Li, S. Kolekar, P.M. Coelho, L. Guo, M. Zhang, Z. Wang, M. Batzill, Synthesis and Characterization of 2D Transition Metal Dichalcogenides: Recent Progress from a Vacuum Surface Science Perspective. Surf. Sci. Rep. 76 (2021) 100523.

[3] J. Kim, C. Bayram, H. Park, C.-W. Cheng, C. Dimitrakopoulos, J.A. Ott, K.B. Reuter, S.W. Bedell, D.K. Sadana, Principle of direct van der Waals epitaxy of single-crystalline films on epitaxial graphene. Nat. Commun. 5 (2014) 4836.

[4] H. Liu, L. Jiao, F. Yang, Y. Cai, X. Wu, W. Ho, C. Gao, J. Jia, N. Wang, H. Fan, W. Yao, M. Xie, Dense network of one-dimensional mid-gap metallic modes in monolayer $MoSe_2$ and their spatial undulations. Phys. Rev. Lett. 113 (2014) 066105.

[5] L. Jiao, H.J. Liu, J.L. Chen, Y. Yi, W.G. Chen, Y. Cai, J.N. Wang, X.Q. Dai, N. Wang, W.K. Ho, M.H. Xie, Molecular-beam epitaxy of monolayer $MoSe_2$: growth characteristics and domain boundary formation. New J. Phys. 17 (2015) 053023.

[6] Y. Ma, H.C. Diaz, J. Avila, C. Chen, V. Kalappattil, R. Das, M.-H. Phan, T. Čadež, J.M.P. Carmelo, M.C. Asensio, M. Batzill, Angle resolved photoemission spectroscopy reveals spin charge separation in metallic $MoSe_2$ grain boundary. Nat. Commun. 8 (2017) 14231.

[7] S. Barja, S. Wickenburg, Z.-F. Liu, Y. Zhang, H. Ryu, M.M. Ugeda, Z. Hussain, Z.-X. Shen, S.-K. Mo, E. Wong, M.B. Salmeron, F. Wang, M.F. Crommie, D.F. Ogletree, J.B. Neaton, A. Weber-Bargioni, Charge density wave order in 1D mirror twin boundaries of single-layer $MoSe_2$. Nat. Phys. 12 (2016) 751–756.

[8] Y. Ma, S. Kolekar, H.C. Diaz, J. Aprojanz, I. Miccoli, C. Tegenkamp, M. Batzill, Metallic twin grain boundaries embedded in $MoSe_2$ monolayers grown by molecular beam epitaxy. ACS Nano 11 (2017) 5130-5139.

[9] J. Chen, G. Wang, Y. Tang, H. Tian, J. Xu, X. Dai H. Xu, J. Jia, W. Ho, M. Xie, Quantum effects and phase tuning in epitaxial hexagonal and monoclinic $MoTe_2$ monolayers. ACS Nano 11 (2017) 3282−3288.

[10] O. Lehtinen, H.-P. Komsa, A. Pulkin, M.B. Whitwick, M.-W. Chen, T. Lehnert, M.J. Mohn, O.V. Yazyev, A. Kis, U. Kaiser, A.V. Krasheninnikov, Atomic scale microstructure and properties of Se-deficient two-dimensional $MoSe_2$. ACS Nano 9 (2015) 3274-3283.

[11] H. Zhu, Q. Wang, L. Cheng, R. Addou, J. Kim, M.J. Kim, R.M. Wallace, Defects and surface structural stability of $MoTe_2$ under vacuum annealing. ACS Nano 11 (2017) 11005-11014.

[12] J. Lin, S.T. Pantelides, W. Zhou, Vacancy-induced formation and growth of inversion domains in transition-metal dichalcogenide monolayer. ACS Nano 9 (2015) 5189–5197.

[13] H.C. Diaz, Y. Ma, R. Chaghi, M. Batzill, High density of (pseudo) periodic twin-grain boundaries in molecular beam epitaxy-grown van der Waals heterostructure: $MoTe_2/MoS_2$. Appl. Phys. Lett. 108 (2016) 191606.

[14] J. Hall, B. Pielić, C. Murray, W. Jolie, T. Wekking, C. Busse, M. Kralj, T. Michely, Molecular beam epitaxy of quasi-freestanding transition metal disulphide monolayers on van der Waals substrates: a growth study. 2D Mater. 5 (2018) 025005.

[15] W. Jolie, C. Murray, P.S. Weiß, J. Hall, F. Portner, N. Atodiresei, A.V. Krasheninnikov, C. Busse, H.-P. Komsa, A. Rosch, T. Michely, Tomonaga-Luttinger liquid in a box: Electrons confined within MoS_2 mirror-twin boundaries. Phys. Rev. X 9 (2019) 011055.

[16] M. Batzill, Mirror twin grain boundaries in molybdenum dichalcogenides. J. Phys.: Condens. Matter 30 (2018) 493001.

[17] P.M. Coelho, H.-P. Komsa, H.C. Diaz, Y. Ma, A.V. Krasheninnikov, M. Batzill, Post-synthesis modifications of two-dimensional $MoSe_2$ or $MoTe_2$ by incorporation of excess metal atoms into the crystal structure. ACS Nano 12 (2018) 3975–3984.

[18] H.-P. Komsa, A.V. Krasheninnikov. Engineering the Electronic Properties of Two-Dimensional Transition Metal Dichalcogenides by Introducing Mirror Twin Boundaries. Adv. Electr. Mater. 6 (2017) 1600468.

[19] Y. Zhang, M.M. Ugeda, C. Jin, S.-F. Shi, A.J. Bradley, A. Martín-Recio, H. Ryu, J. Kim, S. Tang, Y. Kim, B. Zhou, C. Hwang, Y. Chen, F. Wang, M.F. Crommie, Z. Hussain, Z.-X. Shen, S.-K. Mo, Electronic structure, surface doping, and optical response in epitaxial WSe_2 thin films. Nano Lett. 16 (2016) 2485−2491.

[20] H.J. Liu, L. Jiao, L. Xie, F. Yang, J.L. Chen, W.K. Ho, C.L. Gao, J.F. Jia, X.D. Cui, M.H. Xie, Molecular-beam epitaxy of monolayer and bilayer WSe_2: a scanning tunneling microscopy/spectroscopy study and deduction of exciton binding energy. 2D Mater. 2 (2015) 034004.

[21] L.A. Walsh, R. Yue, Q. Wang, A.T. Barton, R. Addou, C.M. Smyth, H. Zhu, J. Kim, L. Colombo, M.J. Kim, R.M Wallace, C.L. Hinkle, WTe_2 thin films grown by beam-interrupted molecular beam epitaxy. 2D Mater. 4 (2017) 025044.

[22] Y.L. Huang, Z. Ding, W. Zhang, Y.-H. Chang, Y. Shi, L.-J. Li, Z. Song, Y.J. Zheng, D. Chi, S.Y. Quek, A.T.S. Wee, Gap states at low-angle grain boundaries in monolayer tungsten diselenide. Nano Lett. 16 (2016) 3682−3688.

[23] J. Karthikeyan, H.P. Komsa, M. Batzill, A.V. Krasheninnikov, Which transition metal atoms can be embedded into two-dimensional molybdenum dichalcogenides and add magnetism? Nano Lett. 19 (2019) 4581-4587.

[24] P.M. Coelho, H.P. Komsa, K. Lasek, V. Kalappattil, J. Karthikeyan, M.H. Phan, A.V. Krasheninnikov, M. Batzill, Room-Temperature Ferromagnetism in $MoTe_2$ by Post-Growth Incorporation of Vanadium Impurities. Adv. Electr. Mater. 5 (2019) 1900044.

[25] T. Kosmala, H.C. Diaz, H.-P. Komsa, Y. Ma, A.V. Krasheninnikov, M. Batzill, and S. Agnoli, Metallic twin boundaries boost the hydrogen evolution reaction on the basal plane of molybdenum selenotellurides. Adv. Ener. Mater. 8 (2018) 1800031.

[26] J. Zhang, Y. Xia, B. Wang, Y. Jin, H. Tian, W.k. Ho, H. Xu, C. Jin, and M. Xie, Single-layer Mo_5Te_8 — A new polymorph of layered transition-metal chalcogenide. 2D Mater. 8 (2021) 015006.

[27] M.V. Bollinger, J.V. Lauritsen, K.W. Jacobsen, J.K. Nørskov, S. Helveg, F. Besenbacher, One-dimensional metallic edge states in MoS_2. Phys. Rev. Lett. 87 (2001) 196803.

[28] M. Gibertini, N. Marzari, Emergence of one-dimensional wires of free carriers in transition metal-dichalcogenide nanostructures. Nano Lett. 15 (2015) 6229−6238.

[29] G. Yang, Y. Shao, J. Niu, X. Ma, C. Lu, W. Wei, X. Chuai, J. Wang, J. Cao, H. Huang, G. Xu, X. Shi, Z. Ji, N. Lu, D. Geng, J. Qi, Y. Cao, Z. Liu, L. Liu, Y. Huang, L. Liao, W. Dang, Z. Zhang, Y. Liu, X. Duan, J. Chen, Z. Fan, X. Jiang, Y. Wang, L. Li, H.-J. Gao, X. Duan, M. Liu, Possible Luttinger liquid behavior of edge transport in monolayer transition metal dichalcogenide crystals. Nat. Commun. 11 (2020) 659.

[30] L. Liu, Z. Ge, C. Yan, A.D. Moghadam, M. Weinert, L. Li, Termination-dependent edge states of MBE-grown WSe_2. Phys. Rev. B 98 (2018) 235304.

[31] P. Mallet, F. Chiapello, H. Okuno, H. Boukari, M. Jamet, J.-Y. Veuillen, Bound Hole States Associated to Individual Vanadium Atoms Incorporated into Monolayer WSe_2. Phys. Rev. Lett. 125 (2020) 036802.

[32] D.L. Duong, S.J. Yun, Y. Kim, S.-G. Kim, Y.H. Lee, Long-range ferromagnetic ordering in vanadium-doped WSe2 semiconductor. Appl. Phys. Lett. 115 (2019) 242406.

[33] S.J. Yun, D.L. Duong, D.M. Ha, K. Singh, T.L. Phan, W. Choi, Y.-M. Kim, Y.H. Lee, Ferromagnetic Order at Room Temperature in Monolayer WSe_2 Semiconductor via Vanadium Dopant. Adv. Sci. 7 (2020) 1903076.

[34] D.L. Duong, S.-G. Kim, Y.H. Lee, Gate modulation of the long-range magnetic order in a vanadium-doped WSe2 semiconductor editors-pick. AIP Advances 10 (2020) 065220.

[35] Y.T.H. Pham, M. Liu, V.O. Jimenez, Z. Yu, V. Kalappattil, F. Zhang, K. Wang, T. Williams, M. Terrones, M.-H. Phan, Tunable Ferromagnetism and Thermally Induced Spin Flip in Vanadium-Doped Tungsten Diselenide Monolayers at Room Temperature. Adv. Mater. 32 (2020) 2003607.

[36] A. Kozhakhmetov, S. Stolz, A.M.Z. Tan, R. Pendurthi, S. Bachu, F. Turker, N. Alem, J. Kachian, S. Das, R.G. Hennig, O. Gröning, B. Schuler, J.A. Robinson, Controllable p-Type Doping of 2D WSe_2 via Vanadium Substitution. Adv. Functional Mater. 31 (2021) 2105252.

[37] S. Fan, S.J. Yun, W.J. Yu, Y.H. Lee, Tailoring Quantum Tunneling in a Vanadium-Doped $WSe_2/SnSe_2$ Heterostructure. Adv. Sci. 7 (2020) 1902751.

[38] S.J. Yun, B.W. Cho, T. Dinesh, D.H. Yang, Y.I. Kim, J.W. Jin, S.-H. Yang, T.D. Nguyen, Y.-M. Kim, K.K. Kim, D.L. Duong, S.-G. Kim, Y.H. Lee, Escalating Ferromagnetic Order via Se-Vacancies Near Vanadium in WSe_2 Monolayers. Adv. Mater. 34 (2022) 2106551.

[39] Y. Murai, S. Zhang, T. Hotta, Z. Liu, T. Endo, H. Shimizu, Y. Miyata, T. Irisawa, Y. Gao, M. Maruyama, S. Okada, H. Mogi, T. Sato, S. Yoshida, H. Shigekawa, T. Taniguchi, K. Watanabe, R. Canton-Vitoria, and R. Kitaura, Versatile Post-Doping toward Two Dimensional Semiconductors. ACS Nano 15 (2021) 19225–19232.

[40] B. Wang, Y. Xia, J. Zhang, H.-P. Komsa, M. Xie, Y. Peng, and C. Jin, Niobium doping induced mirror twin boundaries in MBE grown WSe_2 monolayers. Nano Res. 13 (2020) 1889–1896.